

Bulk phase behaviour vs. interface adsorption: Specific multivalent cation and anion effects on BSA interactions

Madeleine R. Fries,[†] Nina Conzelmann,[†] Luzie Günter,[†] Olga Matsarskaia,[‡]
Maximilian W. A. Skoda,[¶] Robert M. J. Jacobs,[§] Fajun Zhang,[†] and Frank
Schreiber^{*,†,||}

[†]*Institute for Applied Physics, University of Tübingen, 72076 Tübingen, Germany*

[‡]*Institut Max von Laue - Paul Langevin (ILL), CS20156, F-38042, Grenoble, France*

[¶]*Rutherford-Appleton Laboratory, ISIS Facility, Didcot, OX11 0QX, United Kingdom*

[§]*Department for Chemistry, University of Oxford, Oxford, OX1 3TA, United Kingdom*

^{||}*Center for Light-Matter Interaction, Sensors & Analytics LISA⁺, University of Tübingen,
72076 Tübingen, Germany*

E-mail: frank.schreiber@uni-tuebingen.de

Abstract

Proteins are ubiquitous and play a critical role in many areas from living organisms to protein microchips. In humans, serum albumin has a prominent role in the foreign body response since it is the first protein which will interact with e.g. an implant or stent. In this study, we focused on the influence of salts (i.e., different cations (Y^{3+} , La^{3+}) and anions (Cl^- , I^-)) on bovine serum albumin (BSA) in terms of its bulk behaviour, as well as its role of charges for the protein adsorption at the solid-liquid interface in order to understand and control the underlying molecular mechanisms and

interactions. This is part of our group’s effort to gain a deep understanding of protein-protein and protein-surface interactions in the presence of multivalent ions. In the bulk, we found not only multivalent cation-triggered phase transitions, but also a dependence on the anions. The induced attractive interactions were observed to increase from $\text{Cl}^- < \text{NO}_3^- < \text{I}^-$, resulting in iodide preventing re-entrant condensation and promoting liquid-liquid phase separation in bulk. Using ellipsometry and a quartz-crystal microbalance with dissipation (QCM-D), we obtained insight into the growth of the protein adsorption layer thickness. Importantly, we found that phase transitions at the substrate can be triggered by certain interface properties, whether they exist in the bulk solution or not. Through the use of a hydrophilic, negatively charged surface (SiO_2), the direct binding of anions to the interface was prevented. Interestingly, this led to re-entrant adsorption even in the absence of re-entrant condensation in bulk. However, the overall amount of adsorbed protein was enhanced through stronger attractive protein-protein interactions in the presence of iodide salts. These findings illustrate how carefully chosen surface properties and salts can directly steer the binding of anions and cations, which guide protein behaviour, thus paving the way for specific/triggered protein-protein, protein-salt, and protein-surface interactions.

Introduction

Salts are essential for life as we know it. Humans need to ingest adequate amounts of salts *via* their diet¹ in order to maintain biological and physiological functions in the body.² Their absence or excess can ensue diseases such as renal oedema, Addison’s disease, congestive heart failure,² Parkinson’s disease,³ Alzheimer’s⁴ or hypertension.¹ For certain bacteria - called halo bacteria - a high salt concentration is required for survival,⁵ while in plants it can induce cell death due to abiotic stress.⁶

Salts consist of cations and anions, which have different properties and promote ion-specific interactions, thus facilitating different functions in biomolecules, such as proteins,

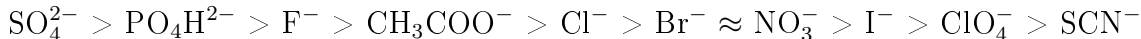
e.g. *via* ion-protein interactions.⁷ To decode their role and more specifically their binding mechanisms to proteins numerous studies were conducted in the past decades.^{8–10} Nevertheless, there are still contradictory opinions and open questions concerning the interplay of electrostatic, hydrophobic, van der Waals and entropic interactions between proteins and salts in bulk and at solid interfaces.

The chloride anion (Cl^-) plays a central role in the human body. It is the body’s principal anion and the second main contributor to blood plasma tonicity¹¹ and has a key role in the regulation of body fluids, the preservation of electrical neutrality, acid-base balance,¹² muscular activity and osmotic pressure.¹¹ In the human body, a chloride imbalance can induce diseases such as dystrophia myotonica, cystic fibrosis, chronic pancreatitis, epilepsy, cataract or Barter’s disease.^{11,13} In addition, it is used to diagnose other diseases and deficiencies.¹⁴ In biopharmaceutical drugs, chloride is, e.g., added to liquid antibody solutions for long-term stability¹⁵ or used to study alcohol degradation in the liver.¹⁶

Another essential anion, which is primarily ingested through fish and dairy products, is iodide (I^-).¹⁷ In the human body, iodine exists in various forms such as I^- , I_2 , I_3 , IO^- , HIO and HI_2O^- .¹⁸ In this study, we focus on I^- . It is most prominently known due to its role in thyroid hormone production,¹⁹ but is also found in saliva, stomach, intestines, kidneys, ovaries and in the blood stream.¹⁸ An iodide deficiency can lead to goitre and hypothyroidism.¹⁸ Especially during pregnancy, an adequate level of iodide is crucial to prevent mental retardation and cretinism in newborns.¹⁸ In medicine, the antioxidant nature of iodide is used to effectively combat free radicals and peroxides. While it is known for its disinfection/antimicrobial properties,²⁰ another important aspect is its positive effect in the treatment of cardio-vascular diseases,²¹ respiratory disorders,²² inflammatory skin diseases, and especially degenerative eye diseases.¹⁷

All of these aspects illustrate the importance of studying protein-ion interactions. These interactions can be estimated with the so-called Hofmeister series.^{23–25} Anions are hereby ordered according to their property of salting-in (stabilising) to salting-out (destabilising)

the protein:



For cations, the corresponding series reads:²⁵



Typical physiologically relevant cations are mostly metal ions and have different valencies from monovalent (e.g. Na^+) to trivalent (e.g. Al^{3+}) ions.²⁶ The trivalent lanthanum cation (La^{3+}), which is less known in the physiological context, can be used on the one hand as a model cation due to its similar size to calcium to study e.g. muscle contraction.²⁷ On the other hand, it can block unwanted bindings of physiological cations with similar size. For example, La^{3+} was found to inhibit the growth of cancerous cells in colon cancer,²⁸ leukaemia²⁹ and skin cancer³⁰ and is thus a component in anticancer drugs already tested *in vivo* and *in vitro*.²⁸ In the same sense, it can act either as a neurotoxin³¹ or trigger the release of neurotransmitters.³² In plants, La^{3+} acts as a chemical fertilizer³³ and relieves the plant of salinity-induced oxidative stress.³⁴

Yttrium (Y) belongs to the group of transition metals, but its chemistry is similar to that of lanthanides.³⁵ Y^{3+} is used in chemotherapy as a treatment for liver cancer³⁶ and in radioimmunotherapy as part of yttrium-labelled antibodies.³⁷ In dentistry, elementary yttrium is incorporated into dental implants for better osteoblast adhesion.³⁸ For a further discussion of multivalent ions, see Ref. 7.

Due to the interaction between opposite charges, cations can bind to negatively charged molecules. Under certain conditions, cations can thereby induce attractive forces e.g. between macro-anions³⁹ and bridge particles of equal charge, such as polyelectrolytes,⁴⁰ surfactants⁴¹ or actin filaments.⁴² Cations can induce charge inversion in biological membranes,⁴³ anionic liposomes⁴⁴ and globular proteins.⁴⁵ Our group observed a complex phase behaviour

for globular proteins (human and bovine serum albumins, beta-lactoglobulin, ovalbumin) in the presence of multivalent cations such as Cd^{2+} , Zn^{2+} , La^{3+} , Al^{3+} , Y^{3+} , Ho^{3+} and Fe^{3+} .^{35,46–50} The phase diagram features phenomena such as liquid-liquid phase separation (LLPS), protein crystallisation, and re-entrant condensation (RC) due to cation-induced charge inversion.^{35,46–50}

In this study, we focus on the effect of anions (Cl^- vs. I^-) and cations (La^{3+} vs. Y^{3+}) on the bulk behaviour of bovine serum albumin (BSA), as well as on its adsorption behaviour on a negatively charged, hydrophilic surface (SiO_2). Serum albumin is often the first protein to adsorb to a solid interface⁵¹ in contact with blood serum. It is the most abundant blood protein and has a well-studied structure⁵² making it an ideal and important protein to study. In terms of substrate properties, hydrophilic surfaces are highly hemocompatible.^{53,54} Negatively charged surfaces are important for initiating blood clotting⁵⁵ by inducing protein adsorption and platelet adhesion,⁵³ besides activating further proteolytic systems in the blood plasma.^{56,57} Thus, SiO_2 is a good model surface to study protein adsorption in addition due to its well-defined properties and smooth surface.

In the following, we shed light on the dominant interactions guiding protein cluster formation and protein adsorption and the influence of multivalent salts on these behaviours. Depending on the ion type, composition and valency, different protein behaviours are observed due to varying type and strength of interactions.

Results and discussion

We studied the effect of different anions and multivalent cations on protein bulk phase behaviour and the adsorption behaviour at a solid-liquid interface. In the following, we will first present the phase behaviour of BSA in the presence of YCl_3 , LaCl_3 , YI_3 and LaI_3 , which differs depending on the anion and cation type in the bulk solution. We aim to obtain a comprehensive picture of the underlying mechanisms and interactions driving these phase

behaviours *via* UV-vis spectroscopy, optical microscopy, Fourier-transform infra-red spectroscopy (FTIR) and pH measurements. Second, we use a net negatively charged, hydrophilic SiO₂ substrate to study protein adsorption by attenuated total reflectance (ATR)-FTIR, ellipsometry and QCM-D measurements. The phase diagrams in the presence of chloride salts were already established in previous publications by Matsarskaia et al.³⁵ and Braun et al.⁵⁸ and are used as a reference for the protein adsorption measurements.

I. Phase diagrams

First, we focus on the anion iodide and its influence on the protein bulk phase behaviour. We establish the phase behaviour of BSA with yttrium iodide (YI₃) and lanthanum iodide (LaI₃) at room temperature in Fig. 1(a,b). Both phase diagrams show a first phase transition from regime I (transparent) into regime II (turbid) at a given salt concentration c^* and a metastable liquid-liquid phase separation (LLPS) region (square symbols in Fig. 1), which starts to form at a protein concentration $c_p \sim 5$ mg/ml, i.e., within regime II. This phase behaviour of globular proteins mixed with multivalent ions has been first established by Zhang et al.⁴⁵ and can be rationalised as follows. The initially net negative charge of the proteins is neutralised by the addition of salt in regime I.^{45,47} At a specific salt concentration c^* , the dominant force changes from repulsive to attractive due to the binding of trivalent cations to negatively charged patches of the protein. The cations can even bridge proteins, thus promoting protein aggregation (regime II).⁵⁹ The protein binding sites of these cations are well studied for HSA.⁶⁰ Due to the similarity of the HSA structure to that of BSA ($\sim 76\%$),^{52,61} comparable binding sites and thus binding mechanisms, of the multivalent cations can be assumed, which are solely defined by acidic (negatively charged) surface-exposed groups. Thus, the binding mechanism between cations and proteins can be rationalised by electrostatic interactions.

In colloid-like systems, including protein solutions, LLPS can occur depending on the interaction strength between particles. One parameter to determine the interaction strength

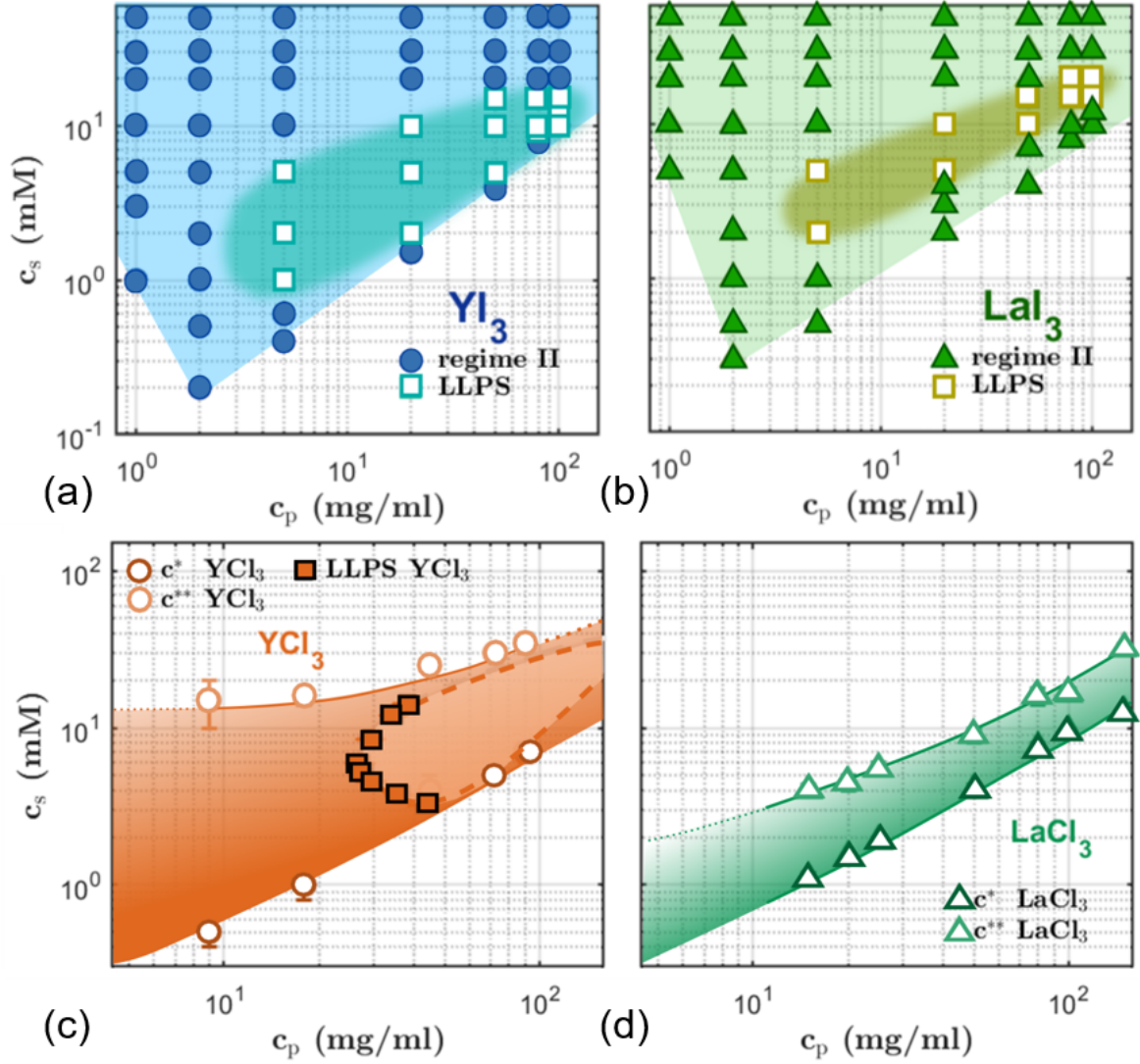


Figure 1: **Phase diagrams.** BSA phase diagrams at room temperature with (a) YI_3 , (b) LaI_3 , (c) YCl_3 and (d) $LaCl_3$. The data in (c) & (d) are modified from Ref. 58. Depending on the salt type, BSA undergoes different phase transitions. All salts, except $LaCl_3$, induce LLPS (square markers). Only the chloride salts lead to re-entrant condensation, whereas BSA in the presence of iodide salts remains in regime II even at high salt concentrations. Note that c^* deviates from a linear slope at very low c_p (1 mg/ml). At low protein concentrations, the intermolecular distances between proteins become very large, thus prohibiting cluster formation until an excessive amount of salt is added.

and type is the reduced second virial coefficient B_2/B_2^{HS} , where B_2^{HS} is the second virial coefficient of hard spheres.⁶² A threshold value of B_2/B_2^{HS} determined for LLPS formation in colloid theory is -1.5.^{62,63} LLPS forms at lower salt concentration (c_s) and extends to higher c_s for BSA with YI_3 than with LaI_3 . In addition, c^* is lower in the presence of YI_3 than LaI_3 .

These differences in BSA phase behaviour induced by Y^{3+} and La^{3+} can be rationalised by weaker protein-protein interactions and cation-protein binding properties of La^{3+} . The cation radius^{64,65} and hydration effects^{66,67} contribute to the effective protein-protein interactions. While other mechanisms may also play a role, it is reasonable to assume that the bigger the cation (lower charge density), the weaker are the attractive interactions it can induce. A detailed study on the role of cations on the BSA phase behaviour was performed by Matsarskaia et al.³⁵ Our findings are consistent with the previous work on chloride salts in Fig. 1 (c)&(d).

Interestingly, no re-entrant condensation occurs with either iodide salt. This implies that no c^{**} into regime III is observed and thus at high c_s , the protein-salt solution remains in regime II. Additionally, in the case of the iodide salts, LLPS begins at lower c_p compared to BSA in the presence of chloride salts in Fig. 1(c)&(d). This indicates there are much stronger BSA-BSA attractive forces in the presence of iodide salts, for which protein-protein interactions are attractive even at very high c_s . This behaviour is in good agreement with the behaviour found for BSA with nitrate salts. Braun et al.⁵⁸ have already observed attractive interaction of BSA at very high c_s , in their case with nitrate salts ($LaNO_3^-$ & YNO_3^-), indicated by the phase diagram and measured B_2/B_2^{HS} values. A systematic change in phase behaviour of BSA with Cl^- , NO_3^- and I^- can be observed: c^* shifts to higher c_s , LLPS occurs at lower c_p and RC vanishes. Thus, ranking the anions from inducing strong attractive interactions from weakest to strongest: $Cl^- < NO_3^- < I^-$. There are multiple factors contributing to this behaviour, which are explained in the following sections and supported by relevant anion properties in Tab. 1.

Table 1: **Properties of anions.** Important parameters, which influence the ion-water and ion-protein interactions relevant for this study.

Parameter	Chloride (Cl ⁻)	Nitrate (NO ₃ ⁻)	Iodide (I ⁻)
Effective anion radius ^{68,69} r_{ion} (Å)	1.81	2.00	2.2
Heat capacity ⁶⁹ $C_{p, str}$ (L/mol)	-237	-234	-288
Ionic aqueous surface tension ⁶⁸ $d\gamma/dc_i$ (nm/m·M)	0.90	0.15	-0.05
Jones-Dole ionic B coefficient ⁶⁹⁻⁷² B (dm ³ /mol)	-0.007	-0.046	-0.068
Number of bound ions to BSA at pH 5 ⁷³ n_{ion} (#)	8	19	48
Structural entropy ^{69,71} S_{str} (J/K·mol)	58	66	117
Water structure parameter ^{68,71,74} ΔG_{HB}	-0.61	-0.68	-1.09

I.1. Hydration and protein stability

According to the Hofmeister series, iodide is more prone to cause destabilisation of the protein (denaturation) than chloride,⁷⁵ which could prevent re-entrant condensation (c^{**}). Yet at low and moderate ionic strengths (<0.1 M), weakly hydrated anions such as iodide neutralise the electrostatic repulsive forces and thermostabilise BSA more efficiently than strongly hydrated anions and are thus more effective stabilisers, leading to the reverse Hofmeister series:⁷⁶⁻⁷⁸

$$\text{SCN}^- > \text{I}^- > \text{NO}_3^- > \text{Br}^- > \text{Cl}^- > \text{SO}_4^{2-}$$

This order is based on the hydration of an ion, which is linked to its ion radius, heat capacity $C_{p, str}$, ionic B coefficient B and structural entropy S_{str} listed in Tab. 1. These properties also determine whether the ion is making or breaking the water structure around itself according to Marcus^{68,69,71} and can be expressed with the water structure parameter ΔG_{HB} .⁷⁴ Thus in this c_s range (<0.1 M), iodide stabilises the BSA structure better than nitrate and nitrate does so better than chloride. In fact, Cl⁻ is known to have little effect on the water structure or protein stability^{79,80} and thus has a passive role in this context.

In order to assess the influence of iodide on the secondary structure of BSA, FTIR measurements were performed (see Fig. 2). The secondary structure of BSA is stable over a LaI₃ concentration range of 0 - 20 mM with a prominent peak around 1650 nm⁻¹ in D₂O

(amide I). This peak is associated with α -helices, which make up roughly 66% of BSA in its native shape⁸¹ and indicates an intact globular structure. Performing multiple measurements at different c_s of 0, 0.4, 3 and 20 mM did not show any significant structural changes in the amide-I band due to salt type or concentration. Thus, we can exclude that denaturation or strong structural changes in the protein structure are the cause for the suppression of re-entrant condensation, i.e. the absence of regime III.

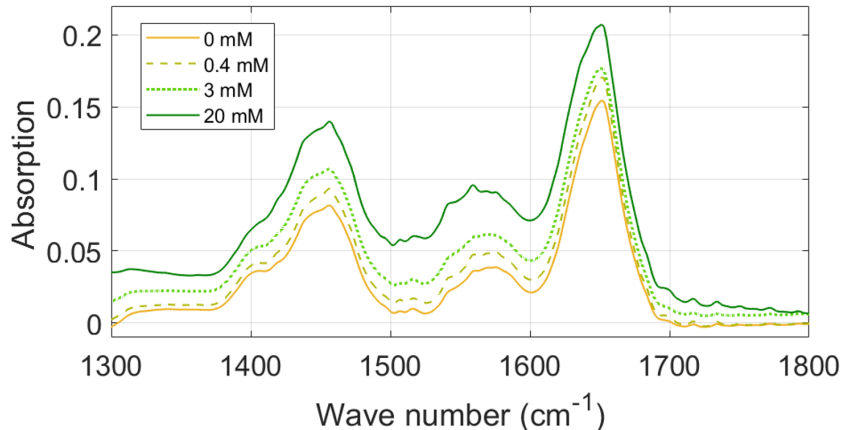


Figure 2: **Secondary structure of BSA.** FTIR transmission measurements of the BSA/LaI₃ system at $c_p = 20$ mg/ml and 20°C in D₂O. The measurements cover all regimes showing no significant changes in the amide-I band (1600-1700 cm⁻¹) at c_s of 0, 0.4, 3 and 20 mM salt. Note that the slight differences in peak intensity and position in amide-II are due to incomplete water subtraction from transmission measurements. The complete FTIR spectra can be found in Fig. S3.

I.2. pH changes

The addition of salt and subsequent salt-induced water hydrolysis and ionisation of hydrophilic protein residues⁸² can change pH and thus, in principle, protein behaviour. Importantly, though, previous studies have shown that the trivalent cations used here do not induce significant pH changes.⁸² To determine the effect of anions on the pH, pH of BSA-LaI₃ samples was measured after preparing the protein/salt mixtures (Fig. 3). The pH decreases slightly with increasing salt concentration, yet the drop in pH does not correlate with the phase transitions seen in the bulk. The pH does not change significantly with time or c_p

either. This pH trend of LaI_3 is similar to that found for YCl_3 .⁸³ We thus conclude that, while pH effects may contribute to the protein phase behaviour in some form, they do not qualitatively change the bulk behaviour and are not primarily responsible for the absence of regime III observed with iodide salts as opposed to the chloride salts.

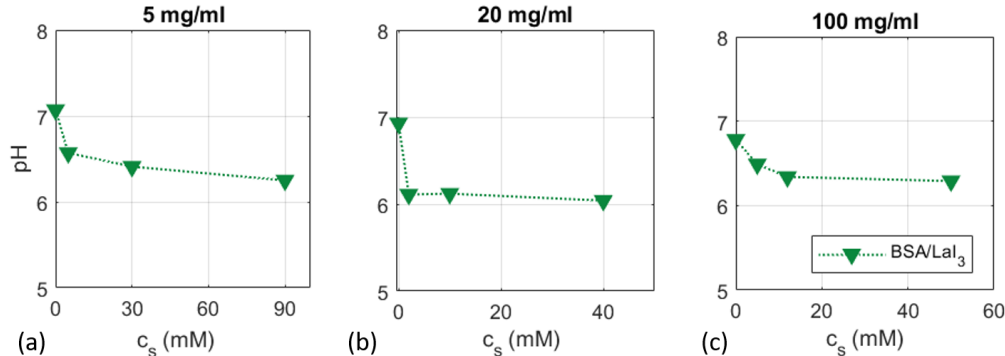


Figure 3: **Bulk pH measurements of the BSA/ LaI_3 system.** at $c_p =$ (a) 5, (b) 20 and (c) 100 mg/ml. The precision of this method can be estimated around $\text{pH} \pm 0.1$.

I.3. Amount of anions bound to BSA.

Literature consistently reports that more iodide anions are bound to BSA per molecule than nitrate ions and even less chloride anions (see Tab. 1).^{73,84} Thus, it is reasonable to assume that iodide has a stronger influence on protein-protein interactions, which again emphasises the general weak effect of Cl^- on the protein stability or water structure.^{79,80} The binding affinity of anions to BSA depends on the properties described in the following sections I.4-I.6.

I.4. Strength of protein-ion interaction.

Weakly hydrated anions bind directly to proteins, causing the protein to maximise its solvent accessible surface area and the bulk solution to become a better solvent.⁸⁵ In turn, strongly hydrated anions interact indirectly through bound water molecules with the protein, thus reducing the proteins surface area by making it more compact. The bulk solution is a bad solvent.⁸⁵ Anions with a lower charge density bind more tightly to the protein. This implies

that iodide binds more tightly to BSA than nitrate and respectively nitrate stronger than chloride (see Tab. 1 for anion radius and surface charge).⁸⁵ In other (positively charged) proteins, it was found that iodide can bridge proteins, thus promoting anion-induced cluster formation.^{86,87} One indicator for iodide-mediated protein-protein bridging, as well as cation bridging of BSA molecules in solution is that at high c_s for both LaI_3 and YI_3 , the protein cluster sizes increase until they start to sediment at $c_s > c_s(\text{LLPS})$ and the volume of 'dense' (sedimented) protein phase further increases with increasing c_s (Fig. S1(a,b)). This is also inversely reflected in the c_p values of the 'dilute' (upper) phase, which decreases with increasing c_p (Fig. S4). The *combination* of increased c_p and volume of the sedimented phase indicates consistently attractive interactions between proteins even at high c_s , preventing re-entrant condensation. The decreased c_p of the dilute phase of YI_3 compared to LaI_3 further supports the finding of stronger BSA-BSA interactions in the presence of Y^{3+} .

I.5. Binding sites.

The literature distinguishes between specific and non-specific, high and low affinity, polar and non-polar ion-binding sites on proteins. It appears to be established that chloride binds to cationic/basic binding sites of BSA^{76,88} and HSA,^{89–91} which are specific and high-affinity binding sites, whereas there are numerous and contradictory opinions on the binding of iodide. Some studies do not discriminate between anion type and thus assume the same binding mechanism for iodide to positively charged protein groups of BSA,^{76,88} while others find a different (non-specific) binding mechanism for iodide to non-polar groups of HSA,⁹¹ lysozyme,^{86,92,93} human carbonic anhydrase II⁹⁴ and peptide.⁹⁵ The same applies to the binding of other anions such as anionic dyes,⁹⁶ anionic amphiphiles⁹⁷ or anionic ligands⁹⁸ to BSA, all of which bind preferentially to hydrophobic groups. In some cases, an interplay of electrostatic and hydrophobic interactions is needed, in which the proximity of positive and non-polar groups has a favourable effect on anion binding.^{91,97,99} BSA has numerous binding sites with different binding affinities due to specific and non-specific binding mechanisms.

In any case, the binding mechanism of iodide is much more complex than the binding of chloride.⁸⁹ Chloride binds only to positively charged sites, whereas, depending on the bulk properties (i.e. charge and polarity of protein), iodide will bind specifically to positively charge sites and/or non-specific to hydrophobic sites with different affinities.

I.6. Competing interactions.

Beside the properties of the anion, the trivalent cations have to be considered as well. Anion-cation chloro-complex formation can be excluded since those start to form at 0.2 M for yttrium salts and 0.4 M for lanthanum salts, respectively.^{100–103} Iodo-complexes start to form at lower c_s than chloro-complexes, yet should not influence our measurements.¹⁰⁴ Thus, anion-cation complexes are almost certainly not contributing to the studied effects. However, anions could assist and amplify the effect of cations on protein-protein interactions.^{95,105} Depending on the cation type and charge of the protein in system, the anion can support the destabilising or stabilising role of the cation on the protein structure.^{95,105}

Overall, electrostatic (and hydrophobic) ion-protein and protein-protein interactions and the special role of multivalent ions are key for the understanding of the observed (bulk) behaviour of iodide salts. The combination of a high number of iodide ions bound to BSA, stronger binding, protein-stabilising role of iodide, potentially anion bridges and non-specific protein-protein interactions, as well as cation bridges, appears to be responsible for preventing the system from undergoing re-entrant condensation triggered by trivalent cations, which means that it remains in regime II with dominant attractive forces between protein molecules.

II. Protein Adsorption

In this section, we discuss how the presence of different salts (LaCl_3 , YCl_3 , LaI_3 , YI_3) in BSA solutions ($c_p = 20$ mg/ml) influences the adsorption behaviour of BSA to a net negatively charged, hydrophilic substrate and to which extent this is related to the bulk protein phase

behaviour.

II.1. Salt-dependent protein adsorption (ellipsometry)

The thickness of the adsorbed amount of BSA on SiO_2 , d , is plotted as a function of ratio of salt/protein concentration (c_s/c_p) in Fig. 4. The effective measured d with ellipsometry assumes a volume fraction of 1, which is laterally averaged over the measured surface.

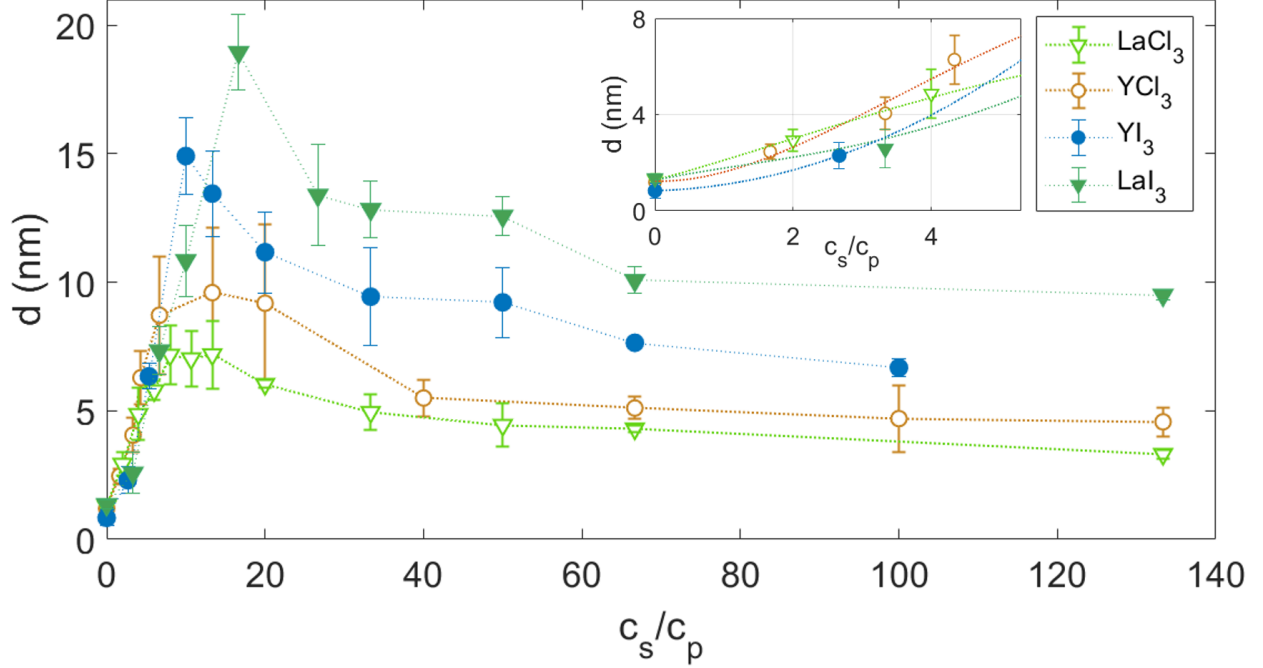


Figure 4: **Ion effect on protein adsorption.** Ellipsometric measurements of the adsorbed protein layer thickness d as a function of c_s/c_p at 20 mg/ml BSA and room temperature for LaCl_3 (light green), YCl_3 (orange), YI_3 (blue) and LaI_3 (dark green). The data for YCl_3 is taken from Ref. 106. The absolute value of d increases as $\text{LaCl}_3 < \text{YCl}_3 < \text{YI}_3 < \text{LaI}_3$. For better visibility, the inset shows a magnification of the initial adsorption increase from 0 to 5 c_s/c_p together with a guide to the eye.

Different aspects need to be considered when comparing the different adsorption trends. These include the position of the adsorption maximum, the amount of protein adsorbed and the overall shape of the curve.

The initial increase of adsorption can be ordered according to the trend $\text{LaI}_3 < \text{LaCl}_3 < \text{YI}_3 < \text{YCl}_3$ shown in the inset of Fig. 4, meaning that the smallest amount of YCl_3 is needed to achieve the thickest adsorption layer at low c_s . This behaviour reflects the bulk phase transition c^*

from regime I to regime II at $2 > 1.5 \approx 1.5 > 1.3$ mM salt, respectively, which occurs at lower c_s for the yttrium salts than for the lanthanum salts due to the stronger attractive inter-protein forces induced by Y^{3+} (see Fig. 1). For iodide salts, more salt has to be added to the protein solution to observe c^* than for chloride salts since iodide has a dominant role in the protein behaviour hindering ‘simple’ charge screening through multivalent cations in bulk and at the interface.

The shape of the adsorption curve maximum is similar to the bulk interactions. In bulk, regime II of the BSA- $LaCl_3$ system is very narrow compared to YCl_3 (Fig. 1(c)), which is reflected in the width of the maximum. For the iodide salts, the LLPS regime starts at a lower c_s (3 mM) for YI_3 than for LaI_3 (5 mM) (Fig. 1(a,b)). This bulk instability induces stronger adsorption explaining the position of the curve maximum in Fig. 4.

Another interesting observable is the maximum adsorbed amount, which follows the order $LaCl_3 < YCl_3 < YI_3 < LaI_3$. The weaker adsorption for $LaCl_3$ in comparison with YCl_3 is due to weaker attractive protein-protein and protein-substrate interactions, which can be explained using the ion-activated attractive adsorption model.¹⁰⁶ It assumes negatively charged patches on the protein and the substrate to which cations can bind and also form ion bridges between protein molecules and between protein and substrate. In this context, we neglect the chloride anions since they have no strong impact on the overall bulk⁸² or adsorption behaviour (as explained in Results section I.) and also, they are obviously the same for $LaCl_3$ and YCl_3 .

The iodide salts show higher maximum adsorption in comparison to the chloride salts. It is important to bear in mind that the iodide salts induce strong LLPS in regime II in the bulk solution (Fig. 1). In a previous publication, we studied the correlation of metastable LLPS formation (bulk instability) in bulk with enhanced protein adsorption⁸³ and found a wetting transition induced by LLPS at the solid interface for BSA with YCl_3 . These results are in good agreement with our findings and further support the wetting layer transition at bulk instability also for iodide salts. Here, LaI_3 leads to more pronounced adsorption compared to YI_3 , which appears counter-intuitive at first. Even though yttrium induces stronger inter-

protein attraction, it appears that this trend is reversed if the counter-ion is iodide. This shows that the ion-activated adsorption model cannot be applied to the iodide salts since the iodide anions compared to chloride ions have a strong impact on the phase behaviour, as well as on adsorption, and the model does not account for the anions in solution. Note that in regime II only the dilute phase can be used for ellipsometer measurements. The dilute phase shows a c_s -dependent decrease in c_p (see Fig. S4). This effect may contribute in some form to the smaller amount of adsorbed protein in the presence of YI_3 compared to LaI_3 , but does not alter the dominant interaction and interaction strength of the bulk solution. It seems that a ‘stronger’ cation such as Y^{3+} induces interactions, which interfere with and hinder the effect of iodide. However, with a ‘weaker’ cation such as La^{3+} , iodide has a more prominent effect on the amount of protein adsorbed, indicating a pronounced formation of anion bridges and non-specific protein-protein binding.

At high c_s , we observe re-entrant adsorption for all salts. For the chloride salts, this was expected since these salts undergo re-entrant condensation at c^{**} from regime II to regime III in bulk, which is defined by charge inversion of the proteins due to trivalent cation binding⁴⁸ and thus a decrease in attractive forces leading to smaller clusters and to a decrease in adsorption. These results are consistent with previous findings in polyelectrolytes¹⁰⁷ and proteins⁸³ and can be explained with the ion-activated adsorption model.¹⁰⁶ For the iodide salts, re-entrant *condensation* in the bulk was not observed. Re-entrant *adsorption* on a solid interface, however, was observed. For a hypothesis on the found behaviour, it helps to consider the possible protein-protein vs. protein-surface interactions. Due to the surface being negatively charged and hydrophilic, anions unlikely bind to the substrate with high surface excess since iodide prefers to adsorb to non-polar and/or positively charged surfaces.^{76,86,88,91,93} This means that in the vicinity of the substrate with restricted properties, charge inversion mediated by trivalent cations can and does occur. In the bulk, in contrast, this is not the case due to the complex protein surface of BSA containing non-polar, polar, negatively and positively charged areas. Consequently, the variety of possible interactions

between protein-protein and protein-salt hinder re-entrant condensation.

II.2. Global protein structure on substrate (ATR-FTIR)

To exclude denaturation at the interface as the primary source for re-entrant adsorption at high c_s , we performed ATR-FTIR measurements on BSA with LaCl_3 and LaI_3 on a Si block (Fig. 5), which showed essentially intact secondary protein structures with both salts with maximum absorbance at 1657 cm^{-1} correlated with its dominant α -helix structure.¹⁰⁸ The absorbance signal is much more intense for LaI_3 , which can be explained by an increased adsorption compared to LaCl_3 and is consistent with the ellipsometry findings. The amide-I band does not significantly change its shape with increasing concentration of the same salt, but it differs slightly between the two salts.

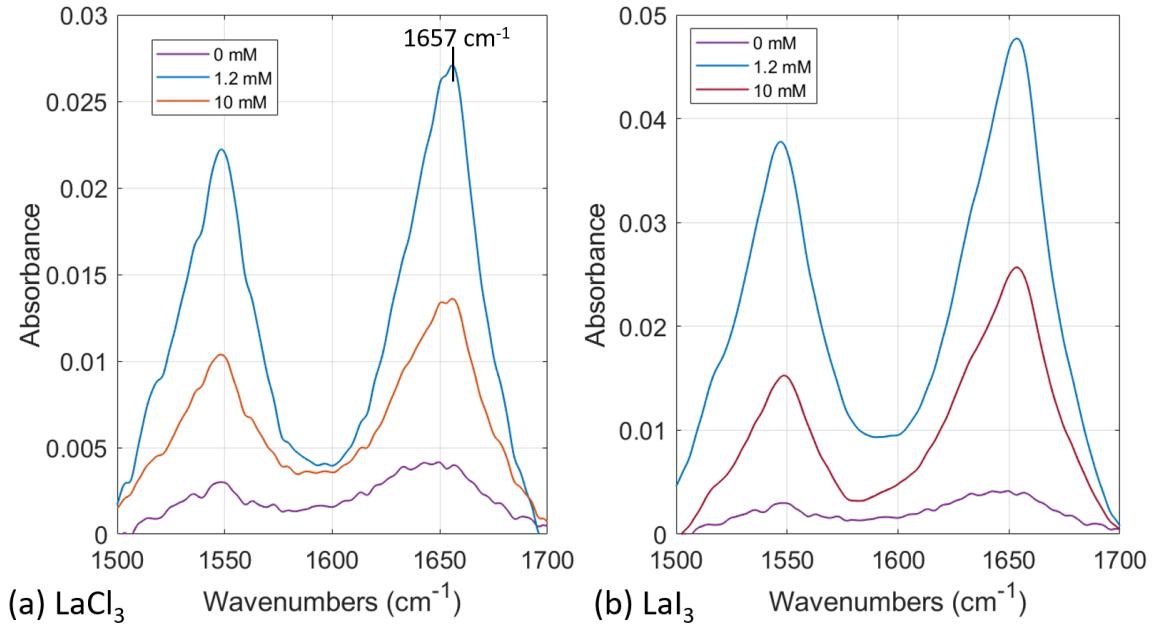


Figure 5: **Structure of adsorption layer.** ATR-FTIR measurements of 5 mg/ml BSA in H_2O on SiO_2 substrates for (a) LaCl_3 and (b) LaI_3 at no salt, 1.2 and 10 mM, respectively.

II.3. Protein layer structure and kinetics (QCM-D)

Complementary measurements were conducted with QCM-D, which on the one hand confirmed the results of our ellipsometry data, and on the other hand provided additional insights into the structure and properties of the adsorption layer.^{109,110} For data analysis, we used the Voigt viscoelastic model^{111–114} to calculate the adsorbed thickness from the measured frequency and dissipation changes (for examples of raw data see Fig. 6). Already from the raw data, the difference between LaCl_3 and LaI_3 is obvious. For all samples in the presence of the respective salt, the frequency drop is lower in the presence of LaI_3 . This means more proteins are adsorbed to the substrate, leading to a stronger damping of the oscillating substrate compared to the same c_s of LaCl_3 . In addition, dissipation is higher in the LLPS regime, indicating a more diffuse layer formation. Similar to the ellipsometry data (Fig. 4), we observe re-entrant adsorption for both data sets. The calculated adsorbed protein layer thickness $d_{\text{QCM-D}}$ is plotted in Fig. 7(a). The overall adsorbed $d_{\text{QCM-D}}$ of BSA/ LaI_3 is enhanced compared to LaCl_3 , which is in good agreement with the results shown in Fig. 4. By rinsing the QCM-D cell with water, the amount of irreversibly adsorbed proteins was determined (Fig. 7, black symbols). These make up only a small portion of the full adsorption layer of roughly 10 nm and can be assumed to be the first monolayer of proteins directly in contact with the substrate.

A big advantage of QCM-D in combination with ellipsometry is that we are able to determine the associated water d_{assoc} within our adsorption model in Fig. 7(b).^{115,116} The associated water consists of a hydration layer around the proteins, hydro-dynamically bound water to the substrate and water trapped within the adsorption layer.¹¹⁷ With the information on the water content in the adsorption layer, the layer morphology can be better understood. In a previous publication,⁸³ we established experimentally and theoretically the correlation between the formation of a wetting layer at the bulk instability induced by LLPS, which exceeded simply ‘stronger adsorption’. Here, only LaI_3 leads to LLPS in regime II and thus induces enhanced adsorption. The calculated associated water content is massively

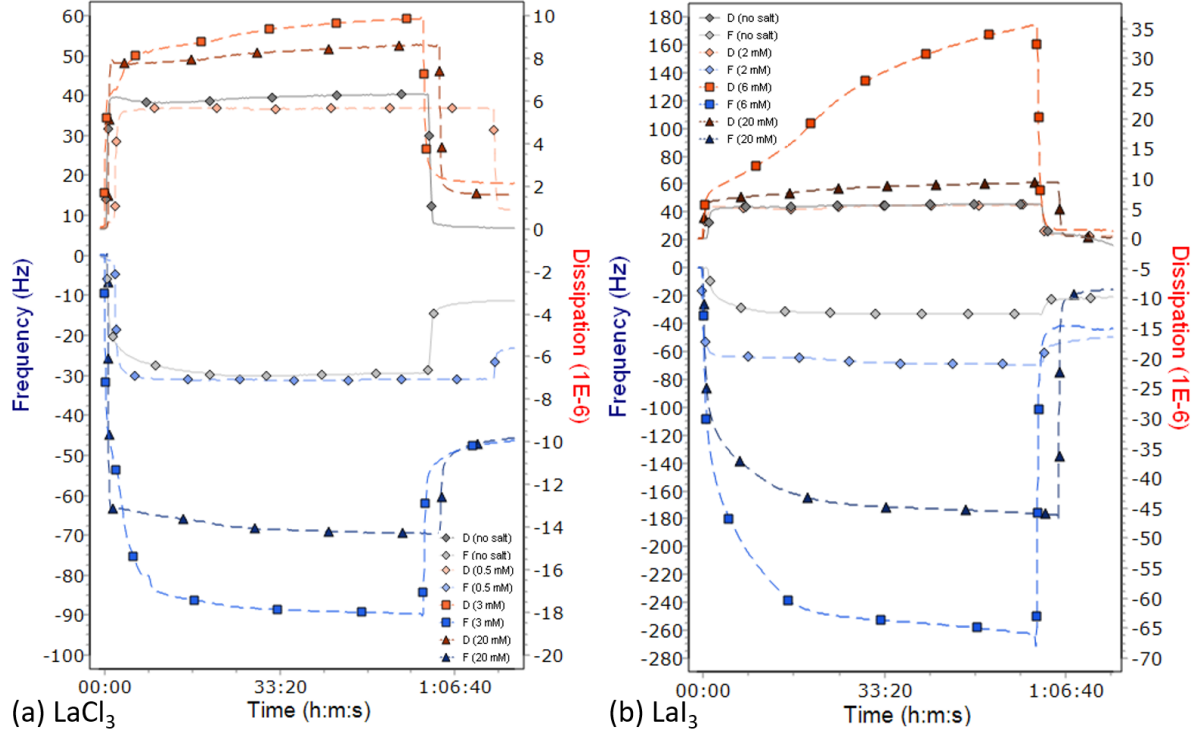


Figure 6: **Real-time adsorption data.** QCM-D frequency and dissipation changes during protein adsorption of 20 mg/ml BSA at room temperature with (a) LaCl_3 and (b) LaI_3 at different c_s reflecting the adsorption behaviour in the different regimes. Note that only the 9th overtone of each measurement is shown for better clarity. Initially, the cell is filled with water, then the protein/salt solution is pumped in and measured for 1h, after which the cell is flushed with water to check for irreversible protein adsorption.

enhanced at $c_s/c_p = 20$, which reflects the onset of a enhanced adsorption (wetting transition) compared to a ‘normal’ adsorption layer in regime I and III and therefore is consistent with our previous findings of BSA/YCl₃.⁸³ This is also reflected in the changed viscoelastic properties and higher water content in the adsorbed protein layer in regime II. Besides this concentration, the water content in the adsorbed layer is comparable between these two salts assuming the same layer morphologies and only enhanced adsorption in the presence of iodide salts.

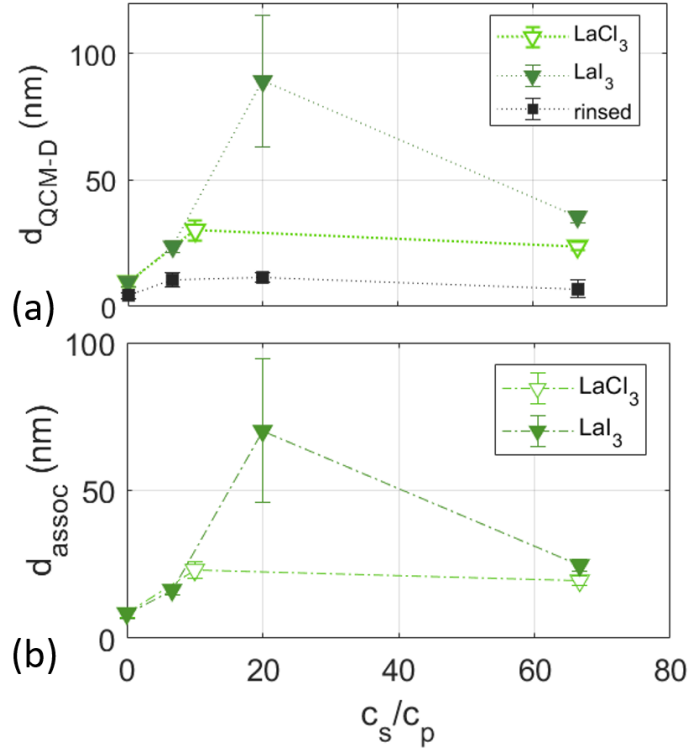


Figure 7: **BSA adsorption with associated water content.** (a) d_{QCM-D} as a function of salt concentration at 20 mg/ml BSA and room temperature for LaCl₃ (light green), LaI₃ (dark green) and rinsed LaI₃ with water (black). (b) Associated water d_{assoc} reflects the water content within the adsorption layer, which is calculated by subtracting the ellipsometer data from the QCM-D data. The enhanced adsorption of LaI₃ is due to a bulk instability (LLPS) and the subsequent formation of a wetting layer. Note that the offset between the two maxima is due to the different positions of regime II in the bulk.

Conclusion

In this study, we focused on the effect of anions and cations on the protein bulk behaviour and adsorption behaviour. Interestingly, we reveal that the co-ion (anion) changes the balance and weakens the effect of trivalent cations in the bulk, making re-entrant condensation disappear and liquid-liquid phase separation appear. Chloride does not appear to affect significantly the phase diagram of BSA, whereas iodide promotes stronger attractive protein-protein interactions.

By choosing specific substrate properties (here: imitating the bulk properties), the influence of ions on protein adsorption can be controlled. In the BSA-YCl₃ system studied in Ref. 106, the bulk and adsorption phase behaviour were highly similar due to similar properties of the proteins, the substrate being net negatively charged and the passive role of chloride. By extending this study to salts with different cations and anions, we have shown that the adsorption behaviour is not solely guided by the dominant electrostatic bulk interactions, but can also be triggered by surface parameters. This explains the observations presented here: re-entrant adsorption in the absence of re-entrant condensation in bulk. The higher adsorbed amount supports the dominant role of iodide and the hypothesis of anion bridging and non-specific binding in bulk.

Through the use of suitable anions and cations, the dominant interactions in bulk can be tuned, while in the adsorption process substrate properties can effectively reduce or even uncouple those interactions. The regulation of interactions on a molecular level opens up new avenues for drug design and biomaterials. In addition to its medical relevance, the use of iodide is potentially very useful for studies of our system using X-rays due to its high scattering power and contrast with light elements (i.e. water and proteins).

Experimental Methods

Materials and bulk phase behaviour

We obtained the materials used in this study from Sigma Aldrich (now Merck), namely BSA with a purity of $\geq 98\%$ (product No. A7906), YCl_3 with a purity of 99.99% (product No. 451363), LaCl_3 with a purity of 99.99% (product No. 449830), YI_3 with a purity of 99.9% (product No. 413011) and LaI_3 with a purity of 99.9% (product No. 413674). Salt stock solutions with a concentration of 100 mM in degassed Milli-Q water were prepared for the bulk and adsorption measurements. BSA has a net negative charge of -10e at neutral pH.⁴⁶ To determine the protein stock solution concentration *via* the Beer-Lambert law, a UV-Vis spectrometer (Cary 50 UV-Vis spectrometer, Varian Technologies, USA) was used to perform absorbance measurements. Most proteins containing aromatic amino acids show an absorption maximum at 280 nm, thus, a range from 200-400 nm was scanned for each concentration determination.

For the phase diagram determination, the protein solutions were prepared with degassed Milli-Q water at c_p of 1, 2, 5, 20, 50, 80 and 100 mg/ml. c_s was varied from 0 to 60 mM. The phase diagrams shown in Fig. 1 were determined by eye, UV-Vis transmission measurements and optical microscopy.⁴⁵ The phase transition c^* is defined by the onset of turbidity (Figs. S1-S2 and Tab. S1) and LLPS by the formation of a dilute and dense liquid phase (Fig. S1(c)). More information is provided in the Supporting Information.

pH measurements were performed with the pH/Ion meter S220 of the Seven Compact series from Mettler Toledo (USA). The error can be estimated to be around $\text{pH} \pm 0.1$ due to deviations in pipetting, concentration determination and electrode precision.

FTIR measurements

FTIR transmission measurements were performed with a Vertex 70 Fourier transform infrared (FTIR) spectrometer by Bruker (software: OPUS) to get insight into the secondary

structure of the protein (clusters) in the different regimes of the bulk solution. We performed a background measurement with the D₂O-filled transmission cell and used the integrated background subtraction tool in OPUS to automatically subtract the background from the sample transmission measurement. The measurements had to be performed in D₂O due to the overlapping absorbance peaks of H₂O with the amide-I band, which we used as an indicator of the integrity of the secondary structure of proteins. Although Braun et al. have found different phase behaviour for protein/salt systems in D₂O vs. H₂O,⁶³ in the present context D₂O was an appropriate solvent to use since it strengthens protein-protein interactions meaning that since we could not observe any structural changes in D₂O, the weaker interactions in H₂O would not induce changes either. The slight difference between pD and pH values of 0.41 does not influence the overall trend of the results found.¹¹⁸

Interface studies/ adsorption

All adsorption measurements were performed *in situ* and the adsorption time was set to 1 h, which was sufficiently close to equilibrium conditions. All samples for ellipsometry and QCM-D were centrifuged and only the supernatant was used (clear solution necessary to perform ellipsometry).

To ensure the reproducibility of our findings and to estimate real standard deviations as statistical error bars, all measurements were repeated at least three times. The systematic errors (e.g. wavelength and angle calibration of the ellipsometer) are substantially smaller than the statistical error bars. In all figures, the mean value of those measurements with real standard deviation is plotted.

Ellipsometry

The substrate was a Si wafer with (111) orientation and a native SiO₂ layer of roughly 1.7 nm on top, which was measured for each sample individually. We utilised a VASE M-2000 ellipsometer by J.A. Woollam (USA) to perform adsorption measurements with a

home-made, solid-liquid cell at 68° , the Brewster angle of SiO_2 in water.^{119–121} For data collection and analysis, we used the CompleteEASE software of J. A. Woollam by creating a model including the optical properties of the individual layers. Specifically for BSA, a Cauchy layer with $A = 1.43$, $B = 0.01$ and $C = 0$ was chosen (in literature the value of A varies from 1.42–1.45 for BSA).^{122–125}

QCM-D measurements

Quartz-crystal microbalance with dissipation (QCM-D) were conducted with the Q-Sense Analyser of Biolin Scientific (Sweden).^{111,126,127} The measurements were performed with the QSoft software and analysed with Dfind and Qtools of Biolin Scientific. The quartz sensors used were SiO_2 -coated (product No. QS-QSX303). The flow cell allowed *in situ* cleaning with 2% Hellmanex, ethanol and water. The set-up had the option of inverted the cell with the substrate on top of the solution, which was utilised, thus avoiding sedimentation effects. Since the dissipation was greater than 0, a viscoelastic (Voigt) model was used for the data analysis of BSA.^{111,128,129} In combination with the ellipsometer, we were able to determine the associated water within our adsorption layer.^{115,116} Since ellipsometry does not account for the water content in d and the QCM-D cannot differentiate between water and proteins adsorbed to the interface, the extracted $d_{\text{QCM-D}}$ contains both. More details on data analysis and fitting parameters can be found in Ref. 83.

ATR-FTIR measurements

ATR-FTIR measurements allow for structure determination of adsorbed proteins to a solid interface and were conducted with the Thermo Nicolet iS50 with Specac Gateway ATR insert.^{130,131} The measurement software was Omnic and the following settings were chosen for the absorbance measurements on Si block: gain: 1, aperture: 10, Scan No. 294, resolution: 4. The evanescent wave penetrates through the substrate a few microns into the bulk solution. Thus, the signal contains the adsorbed proteins, but also the signal of the surrounding

bulk proteins. To check for the influence of the bulk proteins on the absorbance data, we flushed the cell and checked if the signal of the reversibly adsorbed proteins in water is changing compared to the adsorption layer in bulk, which was not the case in Fig. S5. The measurements were conducted in H₂O, but checks were made in D₂O (data not shown), to ensure the background subtraction was sufficient even though the H₂O and amide-I signal are overlapping. The data were corrected for the background, but not for the baseline, which explains the small offset at 0 absorbance of the individual curves in Fig. 5. The slight differences in the amide-II band and amide-I peak position compared to the FTIR measurements in Fig. 2 is due to the use of H₂O as the solvent instead of D₂O.

Acknowledgement

The authors thank Alexander Hinderhofer and Ralph Maier for discussions and the ISIS Biolab in the Rutherford-Appleton Laboratory (Didcot, UK) for giving us access to the ATR-FTIR. Funding by Deutsche Forschungsgemeinschaft and instrument grant by Tübingen University/LISA⁺ is gratefully acknowledged.

Supporting Information Available

The Supporting Information is provided at XXX.

References

- (1) Boegehold, M. A.; Kotchen, T. A. Importance of dietary chloride for salt sensitivity of blood pressure. *Hypertension* **1991**, *17*, I158.
- (2) Grollman, A. The role of salt in health and disease. *The American Journal of Cardiology* **1961**, *8*, 593–601.

- (3) Gaetke, L. M.; Chow, C. K. Copper toxicity, oxidative stress, and antioxidant nutrients. *Toxicology* **2003**, *189*, 147–163.
- (4) Rondeau, V.; Commenges, D.; Jacqmin-Gadda, H.; Dartigues, J.-F. Relation between aluminum concentrations in drinking water and Alzheimer’s disease: an 8-year follow-up study. *American Journal of Epidemiology* **2000**, *152*, 59–66.
- (5) Lanyi, J. K. Salt-dependent properties of proteins from extremely halophilic bacteria. *Bacteriological Reviews* **1974**, *38*, 272.
- (6) Yan, S.; Tang, Z.; Su, W.; Sun, W. Proteomic analysis of salt stress-responsive proteins in rice root. *Proteomics* **2005**, *5*, 235–244.
- (7) Matsarskaia, O.; Roosen-Runge, F.; Schreiber, F. Multivalent ions and biomolecules: Attempting a comprehensive perspective. *ChemPhysChem* **2020**, *n/a*.
- (8) Klotz, I. M.; Urquhart, J. M. The binding of organic ions by proteins. Comparison of native and of modified proteins. *Journal of the American Chemical Society* **1949**, *71*, 1597–1603.
- (9) Lund, M. Anisotropic protein–protein interactions due to ion binding. *Colloids and Surfaces B: Biointerfaces* **2016**, *137*, 17–21.
- (10) Sheinerman, F. B.; Honig, B. On the role of electrostatic interactions in the design of protein–protein interfaces. *Journal of Molecular Biology* **2002**, *318*, 161–177.
- (11) Berend, K.; van Hulsteijn, L. H.; Gans, R. O. Chloride: the queen of electrolytes? *European Journal of Internal Medicine* **2012**, *23*, 203–211.
- (12) Powers, F. The role of chloride in acid-base balance. *Journal of Infusion Nursing* **1999**, *22*, 286.
- (13) Yunos, N. M.; Bellomo, R.; Story, D.; Kellum, J. Bench-to-bedside review: chloride in critical illness. *Critical Care* **2010**, *14*, 226.

- (14) Koch, S. M.; Taylor, R. W. Chloride ion in intensive care medicine. *Critical Care Medicine* **1992**, *20*, 227–240.
- (15) Mason, B. D.; Zhang-van Enk, J.; Zhang, L.; Remmele Jr, R. L.; Zhang, J. Liquid-liquid phase separation of a monoclonal antibody and nonmonotonic influence of Hofmeister anions. *Biophysical Journal* **2010**, *99*, 3792–3800.
- (16) Ward, R. L.; Cull, M. D. Active site chloride binding in liver alcohol dehydrogenase. *Biochimica et Biophysica Acta (BBA)-Protein Structure* **1974**, *365*, 281–284.
- (17) Winkler, R., et al. Iodine—a potential antioxidant and the role of Iodine/Iodide in health and disease. *Natural Science* **2015**, *7*, 548.
- (18) De la Vieja, A.; Santisteban, P. Role of iodide metabolism in physiology and cancer. *Endocrine-related Cancer* **2018**, *25*, R225–R245.
- (19) Ahad, F.; Ganie, S. A. Iodine, iodine metabolism and iodine deficiency disorders revisited. *Indian Journal of Endocrinology and Metabolism* **2010**, *14*, 13.
- (20) Thomas, E. L.; Aune, T. M. Cofactor role of iodide in peroxidase antimicrobial action against *Escherichia coli*. *Antimicrobial Agents and Chemotherapy* **1978**, *13*, 1000–1005.
- (21) Iwata, A.; Morrison, M. L.; Roth, M. B. Iodide protects heart tissue from reperfusion injury. *PloS one* **2014**, *9*.
- (22) Fischer, A. J.; Lennemann, N. J.; Krishnamurthy, S.; Pócza, P.; Durairaj, L.; Launspach, J. L.; Rhein, B. A.; Wohlford-Lenane, C.; Lorentzen, D.; Bánfi, B., et al. Enhancement of respiratory mucosal antiviral defenses by the oxidation of iodide. *American Journal of Respiratory Cell and Molecular Biology* **2011**, *45*, 874–881.
- (23) Moreira, L.; Boström, M.; Ninham, B.; Biscaia, E. C.; Tavares, F. W. Hofmeister effects: Why protein charge, pH titration and protein precipitation depend on the choice

- of background salt solution. *Colloids and Surfaces A: Physicochemical and Engineering Aspects* **2006**, *282*, 457–463.
- (24) Hofmeister, F. Zur Lehre von der Wirkung der Salze. *Naunyn-Schmiedeberg's Archiv für experimentelle Pathologie und Pharmakologie* **1888**, *24*, 247–260.
- (25) Lo Nostro, P.; Ninham, B. W. Hofmeister phenomena: an update on ion specificity in biology. *Chemical Reviews* **2012**, *112*, 2286–2322.
- (26) Williams, R. Tilden Lecture. The biochemistry of sodium, potassium, magnesium, and calcium. *Quarterly Reviews, Chemical Society* **1970**, *24*, 331–365.
- (27) Triggle, C.; Triggle, D. An analysis of the action of cations of the lanthanide series on the mechanical responses of guinea-pig ileal longitudinal muscle. *The Journal of Physiology* **1976**, *254*, 39–54.
- (28) Heffeter, P.; Jakupec, M. A.; Körner, W.; Wild, S.; von Keyserlingk, N. G.; Elbling, L.; Zorbas, H.; Korynevskaya, A.; Knasmüller, S.; Sutterlüty, H., et al. Anticancer activity of the lanthanum compound [tris (1, 10-phenanthroline) lanthanum (III)] trithiocyanate (KP772; FFC24). *Biochemical Pharmacology* **2006**, *71*, 426–440.
- (29) Dai, Y.; Li, J.; Li, J.; Yu, L.; Dai, G.; Hu, A.; Yuan, L.; Wen, Z. Effects of rare earth compounds on growth and apoptosis of leukemic cell lines. *In Vitro Cellular & Developmental Biology-Animal* **2002**, *38*, 373–375.
- (30) Sato, T.; Hashizume, M.; Hotta, Y.; Okahata, Y. Morphology and proliferation of B16 melanoma cells in the presence of lanthanoid and Al³⁺ ions. *Biometals* **1998**, *11*, 107–112.
- (31) Basu, A.; Chakrabarty, K.; Chatterjee, G. C. Neurotoxicity of lanthanum chloride in newborn chicks. *Toxicology Letters* **1982**, *14*, 21–25.

- (32) Vaccari, A.; Saba, P.; Mocci, I.; Ruiu, S. Lanthanides stimulate [3H] tyramine binding in the rat striatum. *Neuroscience Letters* **1999**, *261*, 49–52.
- (33) Palasz, Artur and Czekaj, Piotr, Toxicological and cytophysiological aspects of lanthanides action. *Acta biochimica Polonica* **2000**, *47*, 1107–14.
- (34) Xu, C.-M.; Zhao, B.; Wang, X.-D.; Wang, Y.-C. Lanthanum relieves salinity-induced oxidative stress in *Saussurea involucrata*. *Biologia Plantarum* **2007**, *51*, 567–570.
- (35) Matsarskaia, O.; Roosen-Runge, F.; Lotze, G.; Möller, J.; Mariani, A.; Zhang, F.; Schreiber, F. Tuning phase transitions of aqueous protein solutions by multivalent cations. *Physical Chemistry Chemical Physics* **2018**, *20*, 27214–27225.
- (36) Stubbs, R. S.; Cannan, R. J.; Mitchell, A. W. Selective internal radiation therapy (SIRT) with ⁹⁰Yttrium microspheres for extensive colorectal liver metastases. *Hepato-gastroenterology* **2001**, *48*, 333–337.
- (37) Vaughan, A. T.; Keeling, A.; Yankuba, S. The production and biological distribution of yttrium-90 labelled antibodies. *The International Journal of Applied Radiation and Isotopes* **1985**, *36*, 803–806.
- (38) Webster, T. J.; Ergun, C.; Doremus, R. H.; Bizios, R. Hydroxylapatite with substituted magnesium, zinc, cadmium, and yttrium. II. Mechanisms of osteoblast adhesion. *Journal of Biomedical Materials Research: An Official Journal of The Society for Biomaterials, The Japanese Society for Biomaterials, and The Australian Society for Biomaterials and the Korean Society for Biomaterials* **2002**, *59*, 312–317.
- (39) Fujihara, S.; Akiyama, R. Attractive interaction between macroanions mediated by multivalent cations in biological fluids. *Journal of Molecular Liquids* **2014**, *200*, 89–94.

- (40) Yu, J.; Jackson, N.; Xu, X.; Morgenstern, Y.; Kaufman, Y.; Ruths, M.; De Pablo, J.; Tirrell, M. Multivalent counterions diminish the lubricity of polyelectrolyte brushes. *Science* **2018**, *360*, 1434–1438.
- (41) Wang, X.; Lee, S. Y.; Miller, K.; Welbourn, R.; Stocker, I.; Clarke, S.; Casford, M.; Gutfreund, P.; Skoda, M. W. Cation bridging studied by specular neutron reflection. *Langmuir* **2013**, *29*, 5520–5527.
- (42) Korkmaz Zirpel, N.; Park, E. J. Trivalent Cation Induced Bundle Formation of Filamentous fd Phages. *Macromolecular Bioscience* **2015**, *15*, 1262–1273.
- (43) Gurnev, P. A.; Bezrukov, S. M. Inversion of membrane surface charge by trivalent cations probed with a cation-selective channel. *Langmuir* **2012**, *28*, 15824–15830.
- (44) Martín-Molina, A.; Rodríguez-Beas, C.; Faraudo, J. Charge reversal in anionic liposomes: experimental demonstration and molecular origin. *Physical Review Letters* **2010**, *104*, 168103.
- (45) Zhang, F.; Skoda, M.; Jacobs, R.; Zorn, S.; Martin, R. A.; Martin, C.; Clark, G.; Weggler, S.; Hildebrandt, A.; Kohlbacher, O., et al. Reentrant condensation of proteins in solution induced by multivalent counterions. *Physical Review Letters* **2008**, *101*, 148101.
- (46) Zhang, F.; Skoda, M. W.; Jacobs, R. M.; Martin, R. A.; Martin, C. M.; Schreiber, F. Protein interactions studied by SAXS: effect of ionic strength and protein concentration for BSA in aqueous solutions. *The Journal of Physical Chemistry B* **2007**, *111*, 251–259.
- (47) Zhang, F.; Roosen-Runge, F.; Sauter, A.; Wolf, M.; Jacobs, R. M.; Schreiber, F. Reentrant condensation, liquid–liquid phase separation and crystallization in protein solutions induced by multivalent metal ions. *Pure and Applied Chemistry* **2014**, *86*, 191–202.

- (48) Zhang, F.; Weggler, S.; Ziller, M. J.; Ianeselli, L.; Heck, B. S.; Hildebrandt, A.; Kohlbacher, O.; Skoda, M. W.; Jacobs, R. M.; Schreiber, F. Universality of protein reentrant condensation in solution induced by multivalent metal ions. *Proteins: Structure, Function, and Bioinformatics* **2010**, *78*, 3450–3457.
- (49) Ianeselli, L.; Zhang, F.; Skoda, M. W.; Jacobs, R. M.; Martin, R. A.; Callow, S.; Prévost, S.; Schreiber, F. Protein- protein interactions in ovalbumin solutions studied by small-angle scattering: effect of ionic strength and the chemical nature of cations. *The Journal of Physical Chemistry B* **2010**, *114*, 3776–3783.
- (50) Sauter, A.; Roosen-Runge, F.; Zhang, F.; Lotze, G.; Jacobs, R. M.; Schreiber, F. Real-time observation of nonclassical protein crystallization kinetics. *Journal of the American Chemical Society* **2015**, *137*, 1485–1491.
- (51) Andrade, J.; Hlady, V. *Biopolymers/Non-Exclusion HPLC*; Springer, 1986; pp 1–63.
- (52) Majorek, K. A.; Porebski, P. J.; Dayal, A.; Zimmerman, M. D.; Jablonska, K.; Stewart, A. J.; Chruszcz, M.; Minor, W. Structural and immunologic characterization of bovine, horse, and rabbit serum albumins. *Molecular Immunology* **2012**, *52*, 174–182.
- (53) Sperling, C.; Schweiss, R. B.; Streller, U.; Werner, C. In vitro hemocompatibility of self-assembled monolayers displaying various functional groups. *Biomaterials* **2005**, *26*, 6547–6557.
- (54) Jin, J.; Zhang, C.; Jiang, W.; Luan, S.; Yang, H.; Yin, J.; Stagnaro, P. Melting grafting polypropylene with hydrophilic monomers for improving hemocompatibility. *Colloids and Surfaces A: Physicochemical and Engineering Aspects* **2012**, *407*, 141–149.
- (55) Werner, C.; Maitz, M. F.; Sperling, C. Current strategies towards hemocompatible coatings. *Journal of Materials Chemistry* **2007**, *17*, 3376–3384.

- (56) Colman, R. W.; Schmaier, A. H. Contact system: a vascular biology modulator with anticoagulant, profibrinolytic, antiadhesive, and proinflammatory attributes. *Blood, The Journal of the American Society of Hematology* **1997**, *90*, 3819–3843.
- (57) Colman, R. W. Surface-mediated defense reactions. The plasma contact activation system. *The Journal of Clinical Investigation* **1984**, *73*, 1249–1253.
- (58) Braun, M. K.; Sauter, A.; Matsarskaia, O.; Wolf, M.; Roosen-Runge, F.; Sztucki, M.; Roth, R.; Zhang, F.; Schreiber, F. Reentrant phase behavior in protein solutions induced by multivalent salts: strong effect of anions Cl^- versus NO_3^- . *The Journal of Physical Chemistry B* **2018**, *122*, 11978–11985.
- (59) Roosen-Runge, F.; Zhang, F.; Schreiber, F.; Roth, R. Ion-activated attractive patches as a mechanism for controlled protein interactions. *Scientific Reports* **2014**, *4*, 7016.
- (60) Maier, R.; Zocher, G.; Sauter, A.; Da Vela, S.; Matsarskaia, O.; Schweins, R.; Sztucki, M.; Zhang, F.; Stehle, T.; Schreiber, F. Protein crystallization in the presence of a metastable liquid-liquid phase separation. *in preparation* **2020**,
- (61) Bujacz, A. Structures of bovine, equine and leporine serum albumin. *Acta Crystallographica Section D: Biological Crystallography* **2012**, *68*, 1278–1289.
- (62) Vliegenthart, G.; Lekkerkerker, H. N. Predicting the gas–liquid critical point from the second virial coefficient. *The Journal of Chemical Physics* **2000**, *112*, 5364–5369.
- (63) Braun, M. K.; Wolf, M.; Matsarskaia, O.; Da Vela, S.; Roosen-Runge, F.; Sztucki, M.; Roth, R.; Zhang, F.; Schreiber, F. Strong isotope effects on effective interactions and phase behavior in protein solutions in the presence of multivalent ions. *The Journal of Physical Chemistry B* **2017**, *121*, 1731–1739.
- (64) Schomäcker, K.; Mocker, D.; Münze, R.; Beyer, G.-J. Stabilities of lanthanide-protein

- complexes. *International Journal of Radiation Applications and Instrumentation. Part A. Applied Radiation and Isotopes* **1988**, *39*, 261–264.
- (65) Smolka, G. E.; Birnbaum, E. R.; Darnall, D. W. Rare earth metal ions as substitutes for the calcium ion in *Bacillus subtilis* α -Amylase. *Biochemistry* **1971**, *10*, 4556–4561.
- (66) Gomez, J. E.; Birnbaum, E. R.; Darnall, D. W. Metal ion acceleration of the conversion of trypsinogen to trypsin. Lanthanide ions as calcium ion substitutes. *Biochemistry* **1974**, *13*, 3745–3750.
- (67) Mulqueen, P.; Tingey, J. M.; Horrocks Jr, W. D. Characterization of lanthanide (III) ion binding to calmodulin using luminescence spectroscopy. *Biochemistry* **1985**, *24*, 6639–6645.
- (68) Marcus, Y. Individual ionic surface tension increments in aqueous solutions. *Langmuir* **2013**, *29*, 2881–2888.
- (69) Marcus, Y. Viscosity B-coefficients, structural entropies and heat capacities, and the effects of ions on the structure of water. *Journal of Solution Chemistry* **1994**, *23*, 831–848.
- (70) Jenkins, H. D. B.; Marcus, Y. Viscosity B-coefficients of ions in solution. *Chemical reviews* **1995**, *95*, 2695–2724.
- (71) Marcus, Y. Effect of ions on the structure of water: structure making and breaking. *Chemical reviews* **2009**, *109*, 1346–1370.
- (72) Collins, K. D. Charge density-dependent strength of hydration and biological structure. *Biophysical journal* **1997**, *72*, 65–76.
- (73) Carr, C. W. Studies on the binding of small ions in protein solutions with the use of membrane electrodes. I. The binding of the chloride ion and other inorganic anions

- in solutions of serum albumin. *Archives of Biochemistry and Biophysics* **1952**, *40*, 286–294.
- (74) Marcus, Y. *Ion properties*; CRC Press, 1997.
- (75) Zhang, Y.; Cremer, P. S. Interactions between macromolecules and ions: the Hofmeister series. *Current Opinion in Chemical Biology* **2006**, *10*, 658–663.
- (76) Yamasaki, M.; Yano, H.; Aoki, K. Differential scanning calorimetric studies on bovine serum albumin: II. Effects of neutral salts and urea. *International Journal of Biological Macromolecules* **1991**, *13*, 322–328.
- (77) Cacace, M.; Landau, E.; Ramsden, J. The Hofmeister series: salt and solvent effects on interfacial phenomena. *Quarterly Reviews of Biophysics* **1997**, *30*, 241–277.
- (78) Okur, H. I.; Hladilkova, J.; Rembert, K. B.; Cho, Y.; Heyda, J.; Dzubiella, J.; Cremer, P. S.; Jungwirth, P. Beyond the Hofmeister series: Ion-specific effects on proteins and their biological functions. *The Journal of Physical Chemistry B* **2017**, *121*, 1997–2014.
- (79) Washabaugh, M. W.; Collins, K. D. The systematic characterization by aqueous column chromatography of solutes which affect protein stability. *Journal of Biological Chemistry* **1986**, *261*, 12477–12485.
- (80) Collins, K. D.; Washabaugh, M. W. The Hofmeister effect and the behaviour of water at interfaces. *Quarterly Reviews of Biophysics* **1985**, *18*, 323–422.
- (81) Maruyama, T.; Katoh, S.; Nakajima, M.; Nabetani, H.; Abbott, T. P.; Shono, A.; Satoh, K. FT-IR analysis of BSA fouled on ultrafiltration and microfiltration membranes. *Journal of Membrane Science* **2001**, *192*, 201–207.
- (82) Roosen-Runge, F.; Heck, B. S.; Zhang, F.; Kohlbacher, O.; Schreiber, F. Interplay of

- pH and binding of multivalent metal ions: charge inversion and reentrant condensation in protein solutions. *The Journal of Physical Chemistry B* **2013**, *117*, 5777–5787.
- (83) Fries, M. R.; Stopper, D.; Skoda, M. W.; Blum, M.; Kertzscher, C.; Hinderhofer, A.; Zhang, F.; Jacobs, R. M.; Roth, R.; Schreiber, F. Enhanced protein adsorption upon bulk phase separation. *Scientific reports* **2020**, *10*, 1–9.
- (84) Longworth, L.; Jacobsen, C. An Electrophoretic Study of the Binding of Salt Ions by β -Lactoglobulin and Bovine Serum Albumin. *The Journal of Physical Chemistry* **1949**, *53*, 126–134.
- (85) Collins, K. D. Ions from the Hofmeister series and osmolytes: effects on proteins in solution and in the crystallization process. *Methods* **2004**, *34*, 300–311.
- (86) Vaney, M.; Broutin, I.; Retailleau, P.; Douangamath, A.; Lafont, S.; Hamiaux, C.; Prangé, T.; Ducruix, A.; Riès-Kautt, M. Structural effects of monovalent anions on polymorphic lysozyme crystals. *Acta Crystallographica Section D: Biological Crystallography* **2001**, *57*, 929–940.
- (87) Lund, M.; Jungwirth, P.; Woodward, C. E. Ion specific protein assembly and hydrophobic surface forces. *Physical Review Letters* **2008**, *100*, 258105.
- (88) Scatchard, G.; Coleman, J. S.; Shen, A. L. Physical Chemistry of Protein Solutions. VII. The Binding of Some Small Anions to Serum Albumin. *Journal of the American Chemical Society* **1957**, *79*, 12–20.
- (89) Scatchard, G.; Scheinberg, I. H.; Armstrong Jr, S. H. Physical Chemistry of Protein Solutions. IV. The Combination of Human Serum Albumin with Chloride Ion. *Journal of the American Chemical Society* **1950**, *72*, 535–540.
- (90) Scatchard, G.; Scheinberg, I. H.; Armstrong Jr, S. H. Physical chemistry of protein

- solutions. v. the combination of human serum albumin with thiocyanate ion. *Journal of the American Chemical Society* **1950**, *72*, 540–546.
- (91) Norne, J. E.; Hjalmarsson, S. G.; Lindman, B.; Zeppezauer, M. Anion binding properties of human serum albumin from halide ion quadrupole relaxation. *Biochemistry* **1975**, *14*, 3401–3408.
- (92) Lund, M.; Vácha, R.; Jungwirth, P. Specific ion binding to macromolecules: effects of hydrophobicity and ion pairing. *Langmuir* **2008**, *24*, 3387–3391.
- (93) Lund, M.; Vrbka, L.; Jungwirth, P. Specific ion binding to nonpolar surface patches of proteins. *Journal of the American Chemical Society* **2008**, *130*, 11582–11583.
- (94) Fox, J. M.; Kang, K.; Sherman, W.; Héroux, A.; Sastry, G. M.; Baghbanzadeh, M.; Lockett, M. R.; Whitesides, G. M. Interactions between Hofmeister anions and the binding pocket of a protein. *Journal of the American Chemical Society* **2015**, *137*, 3859–3866.
- (95) Dzubiella, J. Salt-specific stability and denaturation of a short salt-bridge-forming α -helix. *Journal of the American Chemical Society* **2008**, *130*, 14000–14007.
- (96) Karush, F. Heterogeneity of the binding sites of bovine serum albumin. *Journal of the American Chemical Society* **1950**, *72*, 2705–2713.
- (97) Nozaki, Y.; Reynolds, J. A.; Tanford, C. The interaction of a cationic detergent with bovine serum albumin and other proteins. *Journal of Biological Chemistry* **1974**, *249*, 4452–4459.
- (98) Peters Jr, T. *Advances in Protein Chemistry*; Elsevier, 1985; Vol. 37; pp 161–245.
- (99) Rembert, K. B.; Paterova, J.; Heyda, J.; Hilty, C.; Jungwirth, P.; Cremer, P. S. Molecular mechanisms of ion-specific effects on proteins. *Journal of the American Chemical Society* **2012**, *134*, 10039–10046.

- (100) Wood, S. A. The aqueous geochemistry of the rare-earth elements and yttrium: 1. Review of available low-temperature data for inorganic complexes and the inorganic REE speciation of natural waters. *Chemical Geology* **1990**, *82*, 159–186.
- (101) Wood, S. A. The aqueous geochemistry of the rare-earth elements and yttrium: 2. Theoretical predictions of speciation in hydrothermal solutions to 350 C at saturation water vapor pressure. *Chemical Geology* **1990**, *88*, 99–125.
- (102) Rudolph, W. W.; Irmer, G. Hydration and ion pair formation in aqueous Y^{3+} –salt solutions. *Dalton Transactions* **2015**, *44*, 18492–18505.
- (103) Rudolph, W. W.; Irmer, G. Hydration and ion pair formation in common aqueous La (III) salt solutions—a Raman scattering and DFT study. *Dalton Transactions* **2015**, *44*, 295–305.
- (104) Takahashi, R.; Ishiguro, S.-I. Inner-sphere and outer-sphere complexes of yttrium (III), lanthanum (III), neodymium (III), terbium (III) and thulium (III) with halide ions in N, N-dimethylformamide. *Journal of the Chemical Society, Faraday Transactions* **1991**, *87*, 3379–3383.
- (105) Dzubiella, J. Salt-specific stability of short and charged alanine-based α -helices. *The Journal of Physical Chemistry B* **2009**, *113*, 16689–16694.
- (106) Fries, M. R.; Stopper, D.; Braun, M. K.; Hinderhofer, A.; Zhang, F.; Jacobs, R. M.; Skoda, M. W.; Hansen-Goos, H.; Roth, R.; Schreiber, F. Multivalent-ion-activated protein adsorption reflecting bulk reentrant behavior. *Physical Review Letters* **2017**, *119*, 228001.
- (107) Tiraferri, A.; Maroni, P.; Borkovec, M. Adsorption of polyelectrolytes to like-charged substrates induced by multivalent counterions as exemplified by poly (styrene sulfonate) and silica. *Physical Chemistry Chemical Physics* **2015**, *17*, 10348–10352.

- (108) Susi, H.; Byler, D. M. Fourier deconvolution of the amide I Raman band of proteins as related to conformation. *Applied Spectroscopy* **1988**, *42*, 819–826.
- (109) Jordan, J. L.; Fernandez, E. J. QCM-D sensitivity to protein adsorption reversibility. *Biotechnology and Bioengineering* **2008**, *101*, 837–842.
- (110) Rodahl, M.; Höök, F.; Fredriksson, C.; Keller, C. A.; Krozer, A.; Brzezinski, P.; Voinova, M.; Kasemo, B. Simultaneous frequency and dissipation factor QCM measurements of biomolecular adsorption and cell adhesion. *Faraday Discussions* **1997**, *107*, 229–246.
- (111) Voinova, M. V.; Rodahl, M.; Jonson, M.; Kasemo, B. Viscoelastic acoustic response of layered polymer films at fluid-solid interfaces: continuum mechanics approach. *Physica Scripta* **1999**, *59*, 391.
- (112) Voinova, M.; Jonson, M.; Kasemo, B. ‘Missing mass’ effect in biosensor’s QCM applications. *Biosensors and Bioelectronics* **2002**, *17*, 835–841.
- (113) Liu, S. X.; Kim, J.-T. Application of Kelvin—Voigt model in quantifying whey protein adsorption on polyethersulfone using QCM-D. *JALA: Journal of the Association for Laboratory Automation* **2009**, *14*, 213–220.
- (114) Steinem, C.; Janshoff, A. *Piezoelectric sensors*; Springer Science & Business Media, 2007; Vol. 5.
- (115) Macakova, L.; Blomberg, E.; Claesson, P. M. Effect of adsorbed layer surface roughness on the QCM-D response: focus on trapped water. *Langmuir* **2007**, *23*, 12436–12444.
- (116) Rodenhausen, K.; Schubert, M. Virtual separation approach to study porous ultra-thin films by combined spectroscopic ellipsometry and quartz crystal microbalance methods. *Thin Solid Films* **2011**, *519*, 2772–2776.

- (117) Bingen, P.; Wang, G.; Steinmetz, N. F.; Rodahl, M.; Richter, R. P. Solvation effects in the QCM-D response to biomolecular adsorption—a phenomenological approach. *Analytical Chemistry* **2008**, *80*, 8880–8890.
- (118) Covington, A. K.; Paabo, M.; Robinson, R. A.; Bates, R. G. Use of the glass electrode in deuterium oxide and the relation between the standardized pD (paD) scale and the operational pH in heavy water. *Analytical Chemistry* **1968**, *40*, 700–706.
- (119) Mora, M. F.; Wehmeyer, J. L.; Synowicki, R.; Garcia, C. D. *Biological Interactions on Materials Surfaces*; Springer, 2009; pp 19–41.
- (120) Den Boer, J. H. W. G. *Spectroscopic infrared ellipsometry: components, calibration and application*; Technische Universiteit Eindhoven, 1992.
- (121) Cuypers, P.; Hermens, W. T.; Hemker, H. Ellipsometry as a tool to study protein films at liquid-solid interfaces. *Analytical Biochemistry* **1978**, *84*, 56–67.
- (122) Scarangella, A.; Soumbo, M.; Villeneuve-Faure, C.; Mlayah, A.; Bonafos, C.; Monje, M.-C.; Roques, C.; Makasheva, K. Adsorption properties of BSA and DsRed proteins deposited on thin SiO₂ layers: optically non-absorbing versus absorbing proteins. *Nanotechnology* **2018**, *29*, 115101.
- (123) Balevicius, Z.; Paulauskas, A.; Plikusiene, I.; Mikoliunaite, L.; Bechelany, M.; Popov, A.; Ramanavicius, A.; Ramanaviciene, A. Towards the application of Al₂O₃/ZnO nanolaminates in immunosensors: total internal reflection spectroscopic ellipsometry based evaluation of BSA immobilization. *Journal of Materials Chemistry C* **2018**, *6*, 8778–8783.
- (124) Nejadnik, M. R.; Garcia, C. D. Staining proteins: A simple method to increase the sensitivity of ellipsometric measurements in adsorption studies. *Colloids and Surfaces B: Biointerfaces* **2011**, *82*, 253–257.

- (125) Tsargorodskaya, A.; Nabok, A.; Ray, A. Ellipsometric study of the adsorption of bovine serum albumin into porous silicon. *Nanotechnology* **2004**, *15*, 703.
- (126) Reviakine, I.; Johannsmann, D.; Richter, R. P. Hearing what you cannot see and visualizing what you hear: interpreting quartz crystal microbalance data from solvated interfaces. 2011.
- (127) Zhang, B.; Wang, Q. Quartz crystal microbalance with dissipation. *Nanotechnology Research Methods for Food and Bioproducts* **2012**, 181.
- (128) Feiler, A. A.; Sahlholm, A.; Sandberg, T.; Caldwell, K. D. Adsorption and viscoelastic properties of fractionated mucin (BSM) and bovine serum albumin (BSA) studied with quartz crystal microbalance (QCM-D). *Journal of Colloid and Interface Science* **2007**, *315*, 475–481.
- (129) Rojas, E.; Gallego, M.; Reviakine, I. Effect of sample heterogeneity on the interpretation of quartz crystal microbalance data: impurity effects. *Analytical Chemistry* **2008**, *80*, 8982–8990.
- (130) Tantipolphan, R.; Rades, T.; McQuillan, A.; Medicott, N. Adsorption of bovine serum albumin (BSA) onto lecithin studied by attenuated total reflectance Fourier transform infrared (ATR-FTIR) spectroscopy. *International Journal of Pharmaceutics* **2007**, *337*, 40–47.
- (131) Chittur, K. K. FTIR/ATR for protein adsorption to biomaterial surfaces. *Biomaterials* **1998**, *19*, 357–369.

Graphical TOC Entry

